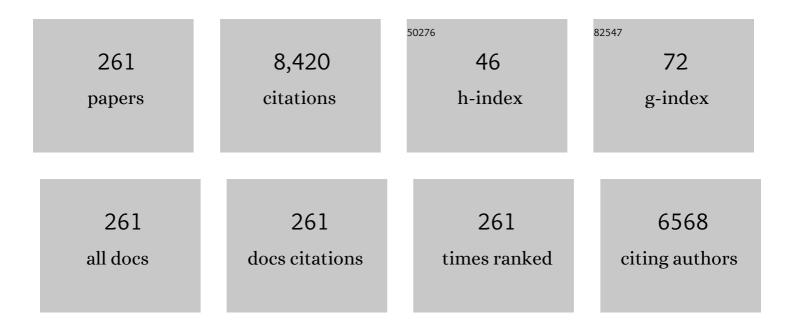
Hc Swart

List of Publications by Year in descending order

Source: https://exaly.com/author-pdf/11619602/publications.pdf Version: 2024-02-01



#	Article	lF	CITATIONS
1	A review on the advancements in phosphor-converted light emitting diodes (pc-LEDs): Phosphor synthesis, device fabrication and characterization. Progress in Materials Science, 2020, 109, 100622.	32.8	373
2	Upconversion based temperature sensing ability of Er3+–Yb3+codoped SrWO4: An optical heating phosphor. Sensors and Actuators B: Chemical, 2015, 209, 352-358.	7.8	355
3	Origin of the red emission in zinc oxide nanophosphors. Materials Letters, 2013, 101, 57-60.	2.6	255
4	Role of film thickness on the properties of ZnO thin films grown by sol-gel method. Thin Solid Films, 2013, 539, 161-165.	1.8	152
5	Enhanced upconversion and temperature sensing study of Er3+–Yb3+ codoped tungsten–tellurite glass. Sensors and Actuators B: Chemical, 2014, 202, 1305-1312.	7.8	152
6	Tunable and white emission from ZnO:Tb3+ nanophosphors for solid state lighting applications. Chemical Engineering Journal, 2014, 255, 541-552.	12.7	146
7	Effect of annealing on the structural, morphological and photoluminescence properties of ZnO thin films prepared by spin coating. Journal of Colloid and Interface Science, 2014, 428, 8-15.	9.4	107
8	Effect of Eu doping on the photoluminescence properties of ZnO nanophosphors for red emission applications. Applied Surface Science, 2014, 308, 419-430.	6.1	105
9	Combustion synthesis and luminescence investigation of Na3Al2(PO4)3:RE (RE = Ce3+, Eu3+ and Mn2+) phosphor. Journal of Alloys and Compounds, 2010, 492, 384-388.	5.5	102
10	Luminescent properties and X-ray photoelectron spectroscopy study of ZnAl2O4:Ce3+,Tb3+ phosphor. Journal of Alloys and Compounds, 2011, 509, 10115-10120.	5.5	93
11	Noble metal nanoparticles embedding into polymeric materials: From fundamentals to applications. Advances in Colloid and Interface Science, 2015, 226, 187-202.	14.7	89
12	Synthesis, spectral and surface investigation of NaSrBO3: Sm3+ phosphor for full color down conversion in LEDs. Journal of Alloys and Compounds, 2013, 554, 214-220.	5.5	84
13	Photoluminescence and phosphorescence properties of MAl2O4:Eu2+, Dy3+ (M=Ca, Ba, Sr) phosphors prepared at an initiating combustion temperature of 500°C. Physica B: Condensed Matter, 2009, 404, 4440-4444.	2.7	83
14	Temperature-dependence on the structural, optical, and paramagnetic properties of ZnO nanostructures. Applied Surface Science, 2014, 293, 62-70.	6.1	82
15	Luminescence dynamics and investigation of Judd-Ofelt intensity parameters of Sm 3+ ion containing glasses. Optical Materials, 2017, 64, 171-178.	3.6	81
16	Review of rare earth activated blue emission phosphors prepared by combustion synthesis. Renewable and Sustainable Energy Reviews, 2015, 52, 596-612.	16.4	76
17	The oxidation of industrial FeCrMo steel. Corrosion Science, 2000, 42, 1725-1740.	6.6	74
18	Photocatalytic and biological applications of Ag and Au doped ZnO nanomaterial synthesized by combustion. Vacuum, 2018, 157, 508-513.	3.5	73

#	Article	IF	CITATIONS
19	Afterglow enhancement with In3+ codoping in CaTiO3:Pr3+ red phosphor. Powder Technology, 2013, 237, 141-146.	4.2	72
20	Synthesis and characterization of Er3+-Yb3+ doped ZnO upconversion nanoparticles for solar cell application. Journal of Alloys and Compounds, 2018, 766, 429-435.	5.5	72
21	In depth study on the notable room-temperature NO2 gas sensor based on CuO nanoplatelets prepared by sonochemical method: Comparison of various bases. Sensors and Actuators B: Chemical, 2018, 266, 761-772.	7.8	69
22	ZnS:Cu,Al,Au phosphor degradation under electron excitation. Applied Surface Science, 1997, 120, 9-14.	6.1	68
23	Effect of Br+6 ions on the structural, morphological and luminescent properties of ZnO/Si thin films. Applied Surface Science, 2013, 279, 472-478.	6.1	68
24	Surface, optical and photocatalytic properties of Rb doped ZnO nanoparticles. Applied Surface Science, 2020, 514, 145930.	6.1	68
25	Gas sensors based on CeO2 nanoparticles prepared by chemical precipitation method and their temperature-dependent selectivity towards H2S and NO2 gases. Applied Surface Science, 2020, 505, 144356.	6.1	67
26	Influence of ultrasonication times on the tunable colour emission of ZnO nanophosphors for lighting applications. Ultrasonics Sonochemistry, 2014, 21, 1549-1556.	8.2	63
27	Effect of Eu3+ on the structure, morphology and optical properties of flower-like ZnO synthesized using chemical bath deposition. Journal of Luminescence, 2014, 147, 85-89.	3.1	62
28	Swift heavy ion irradiation induced modification in structural, optical and luminescence properties of Y2O3:Tb3+ nanophosphor. Journal of Luminescence, 2014, 146, 162-173.	3.1	62
29	Selective detection of CO at room temperature with CuO nanoplatelets sensor for indoor air quality monitoring manifested by crystallinity. Applied Surface Science, 2019, 466, 545-553.	6.1	61
30	Generation of white-light from Dy3+ doped Sr2SiO4 phosphor. Physica B: Condensed Matter, 2014, 439, 126-129.	2.7	60
31	Effects of Cr3+ mol% on the structure and optical properties of the ZnAl2O4:Cr3+ nanocrystals synthesized using sol–gel process. Ceramics International, 2015, 41, 6776-6783.	4.8	60
32	Enhanced UVB emission and analysis of chemical states of Ca5(PO4)3OH:Gd3+,Pr3+ phosphor prepared by co-precipitation. Journal of Physics and Chemistry of Solids, 2014, 75, 998-1003.	4.0	58
33	Embedded plasmonic nanostructures: synthesis, fundamental aspects and their surface enhanced Raman scattering applications. International Reviews in Physical Chemistry, 2016, 35, 353-398.	2.3	58
34	Role of silver doping on the defects related photoluminescence and antibacterial behaviour of zinc oxide nanoparticles. Colloids and Surfaces B: Biointerfaces, 2017, 159, 191-199.	5.0	58
35	Potential of Sm 3+ doped LiSrVO 4 nanophosphor to fill amber gap in LEDs. Physica B: Condensed Matter, 2018, 535, 221-226.	2.7	57
36	A near-UV-converted LiMgBO3:Dy3+ nanophosphor: Surface and spectral investigations. Applied Surface Science, 2015, 329, 40-46.	6.1	53

#	Article	IF	CITATIONS
37	Infrared emission spectroscopy and upconversion of ZnO-Li2O-Na2O-P2O5 glasses doped with Nd3+ ions. Journal of Non-Crystalline Solids, 2017, 457, 157-163.	3.1	53
38	A comparative study on structural, morphological and luminescence characteristics of Zn3(VO4)2 phosphor prepared via hydrothermal and citrate-gel combustion routes. Physica B: Condensed Matter, 2012, 407, 1485-1488.	2.7	52
39	Luminescence of Ce doped MgAl2O4 prepared by the combustion method. Physica B: Condensed Matter, 2014, 439, 109-114.	2.7	52
40	The role of oxygen and titanium related defects on the emission of TiO2:Tb3+ nano-phosphor for blue lighting applications. Optical Materials, 2015, 46, 510-516.	3.6	52
41	The difference in degradation behaviour of ZnS:Cu,Al,Au and ZnS:Ag,Cl phosphor powders. Applied Surface Science, 1999, 140, 63-69.	6.1	51
42	Enhanced luminescence and degradation of SiO2:Ce,Tb powder phosphors prepared by a sol–gel process. Journal of Physics and Chemistry of Solids, 2006, 67, 1749-1753.	4.0	50
43	Investigations on the low voltage cathodoluminescence stability and surface chemical behaviour using Auger and X-ray photoelectron spectroscopy on LiSrBO3:Sm3+ phosphor. Materials Research Bulletin, 2011, 46, 987-994.	5.2	50
44	Spectroscopic studies of Sm3+/Dy3+ co-doped lithium boro-silicate glasses. Journal of Non-Crystalline Solids, 2016, 438, 49-58.	3.1	50
45	Transparent conducting ZnO-CdO mixed oxide thin films grown by the sol-gel method. Journal of Colloid and Interface Science, 2017, 487, 378-387.	9.4	50
46	Defects induced enhancement of antifungal activities of Zn doped CuO nanostructures. Applied Surface Science, 2021, 560, 150026.	6.1	50
47	Resolution of Eu2+ asymmetrical emission peak of SrAl2O4:Eu2+, Dy3+ phosphor by cathodoluminescence measurements. Materials Letters, 2008, 62, 3192-3194.	2.6	47
48	Luminescence investigations of Ce3+ doped CaS nanophosphors. Journal of Alloys and Compounds, 2010, 492, L8-L12.	5.5	47
49	Influence of Ag, Au and Pd noble metals doping on structural, optical and antimicrobial properties of zinc oxide and titanium dioxide nanomaterials. Heliyon, 2019, 5, e01333.	3.2	47
50	Synthesis and characterization of Ce3+ doped silica (SiO2) nanoparticles. Journal of Luminescence, 2011, 131, 1249-1254.	3.1	46
51	Synthesis and characterization of BaAl2O4:Eu2+ co-doped with different rare earth ions. Physica B: Condensed Matter, 2012, 407, 1603-1606.	2.7	46
52	Effect of annealing on the structural, morphological and optical properties of Ga-doped ZnO nanoparticles by reflux precipitation method. Results in Physics, 2017, 7, 2022-2027.	4.1	46
53	X-ray photoelectron spectroscopy and luminescent properties of Y2O3:Bi3+ phosphor. Applied Surface Science, 2015, 332, 198-204.	6.1	45
54	Enhancement of upconversion emission and temperature sensing of paramagnetic Gd2Mo3O9: Er3+/Yb3+ phosphor via Li+/Mg2+ co-doping. Journal of Alloys and Compounds, 2018, 747, 455-464.	5.5	45

#	Article	IF	CITATIONS
55	Eu 3+ doped down shifting TiO 2 layer for efficient dye-sensitized solar cells. Journal of Colloid and Interface Science, 2016, 484, 24-32.	9.4	44
56	Influence of Bi doping on the structure and photoluminescence of ZnO phosphor synthesized by the combustion method. Spectrochimica Acta - Part A: Molecular and Biomolecular Spectroscopy, 2018, 190, 164-171.	3.9	44
57	Defect-induced magnetism in undoped and Mn-doped wide band gap zinc oxide grown by aerosol spray pyrolysis. Applied Surface Science, 2014, 311, 14-26.	6.1	43
58	Structural and luminescence properties of Eu3+/Dy3+ embedded sodium silicate glass for multicolour emission. Journal of Alloys and Compounds, 2017, 708, 922-931.	5.5	43
59	Roles of doping ions in afterglow properties of blue CaAl2O4:Eu2+,Nd3+ phosphors. Physica B: Condensed Matter, 2014, 439, 153-159.	2.7	42
60	Characteristics of the mechanical milling on the room temperature ferromagnetism and sensing properties of TiO2 nanoparticles. Applied Surface Science, 2015, 331, 362-372.	6.1	42
61	ZnS thin films grown on Si(100) by XeCl pulsed laser ablation. Applied Surface Science, 2001, 177, 73-77.	6.1	41
62	CaTiO3:Eu3+, a potential red long lasting phosphor: Energy migration and characterization of trap level distribution. Journal of Alloys and Compounds, 2015, 622, 1068-1073.	5.5	41
63	Charge compensated derived enhanced red emission from Sr 3 (VO 4) 2 :Eu 3+ nanophosphors for white light emitting diodes and flat panel displays. Journal of Alloys and Compounds, 2017, 709, 362-372.	5.5	41
64	Preparation and characterization of Ce doped ZnO nanomaterial for photocatalytic and biological applications. Materials Science and Engineering B: Solid-State Materials for Advanced Technology, 2020, 261, 114780.	3.5	41
65	Effect of alkali metal ions (Li+, Na+ and K+) on the luminescence properties of CaMgB2O5: Sm3+ nanophosphor. Nano Structures Nano Objects, 2015, 3, 9-16.	3.5	40
66	Combustion synthesis and characterization of blue long lasting phosphor CaAl 2 O 4 : Eu 2+ , Dy 3+ and its novel application in latent fingerprint and lip mark detection. Physica B: Condensed Matter, 2018, 535, 149-156.	2.7	40
67	Effects of cationic substitution on the luminescence behavior of Dy3+ doped orthophosphate phosphor. Journal of Alloys and Compounds, 2019, 806, 1127-1137.	5.5	40
68	The effects of Eu-concentrations on the luminescent properties of SrF 2 :Eu nanophosphor. Journal of Luminescence, 2014, 156, 150-156.	3.1	39
69	Characterization of annealed Eu 3+ -doped ZnO flower-like morphology synthesized by chemical bath deposition method. Optical Materials, 2016, 60, 294-304.	3.6	39
70	Spectroscopic properties of Pr3+ ions embedded in lithium borate glasses. Physica B: Condensed Matter, 2016, 480, 111-115.	2.7	39
71	Optical and surface properties of Zn doped CdO nanorods and antimicrobial applications. Colloids and Surfaces A: Physicochemical and Engineering Aspects, 2020, 605, 125369.	4.7	39
72	Structural and spectral studies of highly pure red-emitting Ca3B2O6:Eu3+ phosphors for white light emitting diodes. Journal of Alloys and Compounds, 2021, 869, 159363.	5.5	39

#	Article	IF	CITATIONS
73	The effect of Ce3+ on structure, morphology and optical properties of flower-like ZnO synthesized using the chemical bath method. Journal of Luminescence, 2013, 143, 463-468.	3.1	37
74	Properties of flower-like ZnO nanostructures synthesized using the chemical bath deposition. Materials Science in Semiconductor Processing, 2014, 27, 33-40.	4.0	37
75	Low voltage electron induced cathodoluminescence degradation and surface characterization of Sr3(PO4)2:Tb phosphor. Applied Surface Science, 2011, 257, 10147-10155.	6.1	36
76	Surface state of Y3(Al,Ga)5O12:Tb phosphor under electron beam bombardment. Applied Surface Science, 2012, 258, 6495-6503.	6.1	36
77	Phosphorescent and thermoluminescent properties of SrAl2O4:Eu2+, Dy3+ phosphors prepared by solid state reaction method. Physica B: Condensed Matter, 2012, 407, 1679-1682.	2.7	36
78	Characterization and luminescent properties of SiO2:ZnS:Mn2+ and ZnS:Mn2+ nanophosphors synthesized by a sol–gel method. Physica B: Condensed Matter, 2009, 404, 4470-4475.	2.7	35
79	Luminescence investigations on LiAl5O8:Tb3+ nanocrystalline phosphors. Current Applied Physics, 2011, 11, 341-345.	2.4	35
80	Effect of annealing temperature on structural and optical properties of ZnAl 2 O 4 :1.5% Pb 2+ nanocrystals synthesized via sol-gel reaction. Journal of Alloys and Compounds, 2016, 677, 72-79.	5.5	35
81	Structural, surface and luminescence properties of Ca3B2O6:Dy3+ phosphors. Ceramics International, 2016, 42, 5743-5753.	4.8	35
82	A comparative investigation on ion impact parameters and TL response of Y2O3:Tb3+ nanophosphor exposed to swift heavy ions for space dosimetry. Journal of Alloys and Compounds, 2014, 589, 5-18.	5.5	34
83	Electrical and optical properties of p-type codoped ZnO thin films prepared by spin coating technique. Physica E: Low-Dimensional Systems and Nanostructures, 2016, 77, 1-6.	2.7	34
84	Improved steady-state photoluminescence derived from the compensation of the charge-imbalance in Ca3Mg3(PO4)4:Eu3+ phosphor. Ceramics International, 2019, 45, 21709-21715.	4.8	34
85	Luminescence characterization and electron beam induced chemical changes on the surface of ZnAl2O4:Mn nanocrystalline phosphor. Applied Surface Science, 2011, 257, 3298-3306.	6.1	33
86	The greenish-blue emission and thermoluminescent properties of CaTa2O6:Pr3+. Journal of Alloys and Compounds, 2014, 589, 88-93.	5.5	33
87	Enhanced exciton emission from ZnO nano-phosphor induced by Yb3+ ions. Materials Letters, 2014, 119, 71-74.	2.6	33
88	Comparison and analysis of Eu3+ luminescence in Y3Al5O12 and Y3Ga5O12 hosts material for red lighting phosphor. Materials Chemistry and Physics, 2015, 166, 167-175.	4.0	33
89	Tailoring and optimization of optical properties of CdO thin films for gas sensing applications. Physica B: Condensed Matter, 2018, 535, 314-318.	2.7	33
90	Electron beam induced degradation of a pulsed laser deposited ZnS:Cu,Au,Al thin film on a Si(1 0 0) substrate. Applied Surface Science, 2001, 183, 304-310.	6.1	32

#	Article	IF	CITATIONS
91	Role of swift heavy ions irradiation on the emission of boron doped ZnO thin films for near white light application. Journal of Alloys and Compounds, 2014, 594, 32-38.	5.5	32
92	Luminescent properties, intensity degradation and X-ray photoelectron spectroscopy analysis of CaS:Eu2+ powder. Optical Materials, 2015, 40, 68-75.	3.6	32
93	(INVITED) Ultraviolet and visible luminescence from bismuth doped materials. Optical Materials: X, 2019, 2, 100025.	0.8	32
94	Multifunction applications of Bi2O3:Eu3+ nanophosphor for red light emission and photocatalytic activity. Applied Surface Science, 2019, 497, 143748.	6.1	32
95	Structural, optical and photoluminescence properties of Eu doped ZnO thin films prepared by spin coating. Journal of Molecular Structure, 2019, 1192, 105-114.	3.6	32
96	H2S detection capabilities with fibrous-like La-doped ZnO nanostructures: A comparative study on the combined effects of La-doping and post-annealing. Journal of Alloys and Compounds, 2019, 797, 284-301.	5.5	32
97	Dependence of Eu3+ luminescence dynamics on the structure of the combustion synthesized Sr5(PO4)3F host. Journal of Alloys and Compounds, 2011, 509, 2544-2551.	5.5	31
98	Synthesis and optical studies of KCaVO4:Sm3+/PMMA nanocomposites. Vacuum, 2019, 159, 414-422.	3.5	31
99	Photoluminescence and thermoluminescence properties of Pr3+ doped ZnTa2O6 phosphor. Powder Technology, 2013, 247, 147-150.	4.2	30
100	Conversion of Y3(Al,Ga)5O12:Tb3+ to Y2Si2O7:Tb3+ thin film by annealing at higher temperatures. Applied Surface Science, 2013, 270, 331-339.	6.1	30
101	NaSrVO4:Sm3+ â^ An n-UV convertible phosphor to fill the quantum efficiency gap for LED applications. Ceramics International, 2016, 42, 2317-2323.	4.8	29
102	Luminescence properties of Bi doped La2O3 powder phosphor. Journal of Luminescence, 2019, 209, 217-224.	3.1	29
103	Electron beam-induced degradation of zinc sulfide-based phosphors. Surface Science, 2000, 451, 174-181.	1.9	28
104	Photon upconversion in Ho3+-Yb3+ embedded tungsten tellurite glass. Journal of Luminescence, 2017, 192, 757-760.	3.1	28
105	Multifunctional properties of plasmonic Cu nanoparticles embedded in a glass matrix and their thermodynamic behavior. Journal of Alloys and Compounds, 2018, 747, 530-542.	5.5	28
106	Effects of octadecylammine molar concentration on the structure, morphology and optical properties of ZnO nanostructure prepared by homogeneous precipitation method. Journal of Luminescence, 2018, 200, 206-215.	3.1	28
107	Facile precipitation synthesis of green-emitting BaY2F8:Yb3+, Ho3+ upconverting phosphor. Ceramics International, 2019, 45, 14205-14213.	4.8	28
108	Extracting inter-diffusion parameters of TiC from AES depth profiles. Applied Surface Science, 2003, 205, 231-239.	6.1	27

#	Article	IF	CITATIONS
109	Luminescent properties of Ca0.97Al2O4:Eu0.012+,Dy0.023+ phosphors prepared by combustion method at different initiating temperatures. Journal of Alloys and Compounds, 2010, 508, 262-265.	5.5	27
110	PL and CL degradation and characteristics of SrAl2O4: Eu2+,Dy3+ phosphors. Physica B: Condensed Matter, 2012, 407, 1664-1667. Condense and charge charge can be a start of the second star	2.7	27
111	x% 16 3+ <mml:math si1.gif<br="" xmlns:mml="http://www.w3.org/1998/Wath/WathWL_altimg=">overflow="scroll"><mml:mrow><mml:mo< td=""><td></td><td></td></mml:mo<></mml:mrow></mml:math>		

#	Article	IF	CITATIONS
127	The effect of different gas atmospheres on luminescent properties of pulsed laser ablated SrAl2O4:Eu2+,Dy3+ thinfilms. Journal of Luminescence, 2011, 131, 119-125.	3.1	22
128	Charge compensated CaSr2(PO4)2:Sm3+, Li+/Na+/K+ phosphor: Luminescence and thermometric studies. Journal of Alloys and Compounds, 2022, 901, 163793.	5.5	22
129	Concentration quenching, surface and spectral analyses of SrF2:Pr3+ prepared by different synthesis techniques. Optical Materials, 2015, 42, 204-209.	3.6	21
130	Energy transfer study between Ce 3+ and Tb 3+ ions in a calcium fluoride crystal for solar cell applications. Journal of Luminescence, 2017, 187, 96-101.	3.1	21
131	Surface and spectral studies of Sm3+ doped Li4Ca(BO3)2 phosphors for white light emitting diodes. Journal of Alloys and Compounds, 2018, 738, 97-104.	5.5	21
132	Pulsed laser deposition of a ZnO:Eu3+ thin film: Study of the luminescence and surface state under electron beam irradiation. Applied Surface Science, 2020, 502, 144281.	6.1	21
133	Effect of a CdO coating on the degradation of a ZnS thin film phosphor material. Applied Surface Science, 2002, 187, 137-144.	6.1	20
134	Degradation of Y2SiO5:Ce phosphor powders. Journal of Luminescence, 2007, 126, 37-42.	3.1	20
135	The effect of Mg2+ ions on the photoluminescence of Ce3+-doped silica. Physica B: Condensed Matter, 2009, 404, 4499-4503.	2.7	20
136	The cathodoluminescence degradation and surface characterization of β-Ca3(PO4)2:Tb phosphor. Optical Materials, 2012, 34, 1398-1405.	3.6	20
137	A study on the sensing of NO2 and O2 utilizing ZnO films grown by aerosol spray pyrolysis. Materials Chemistry and Physics, 2015, 162, 628-639.	4.0	20
138	Temperature induced upconversion behaviour of Ho3+-Yb3+ codoped yttrium oxide films prepared by pulsed laser deposition. Journal of Alloys and Compounds, 2016, 672, 190-196.	5.5	20
139	Effect of PLD growth atmosphere on the physical properties of ZnO:Zn thin films. Optical Materials, 2017, 74, 76-85.	3.6	20
140	Surface characterization and cathodoluminescence degradation of ZnO thin films. Applied Surface Science, 2017, 424, 412-420.	6.1	20
141	Investigation of thermoluminescence response and trapping parameters of 120ÂMeV Ag9+ and γ-ray exposed NaSrBO3:Dy3+ phosphor for dosimetry. Journal of Alloys and Compounds, 2017, 691, 919-928.	5.5	20
142	Cathodoluminescent stability of rare earth tantalate phosphors. Journal of Luminescence, 2013, 140, 14-20.	3.1	19
143	Radiative energy transfer in ZnAl2O4:0.1% Ce3+, x% Eu3+ nanophosphor synthesized by sol–gel process. Physica B: Condensed Matter, 2015, 468-469, 11-20.	2.7	19
144	Effect of doping concentration on the conductivity and optical properties of p-type ZnO thin films. Physica B: Condensed Matter, 2016, 480, 31-35.	2.7	19

#	Article	IF	CITATIONS
145	Synthesis, structure and optical studies of ZnO:Eu3+,Er3+,Yb3+ thin films: Enhanced up-conversion emission. Colloids and Surfaces A: Physicochemical and Engineering Aspects, 2018, 540, 123-135.	4.7	19
146	Structural and luminescence properties of thermally stable cool-white light emitting NaCaPO4:Dy3+ phosphor. Optik, 2020, 219, 165026.	2.9	19
147	Synthesis, surface and photoluminescence properties of Sm3+ doped α-Bi2O3. Journal of Alloys and Compounds, 2021, 854, 157221.	5.5	19
148	Auger electron/X-ray photoelectron and cathodoluminescent spectroscopic studies of pulsed laser ablated SrAl2O4:Eu2+,Dy3+ thin films. Applied Surface Science, 2010, 257, 512-517.	6.1	18
149	Thermoluminescence of calcium phosphate co-doped with gadolinium and praseodymium. Radiation Measurements, 2015, 77, 26-33.	1.4	18
150	Effect of substrate temperature and post annealing temperature on ZnO:Zn PLD thin film properties. Optical Materials, 2017, 74, 139-149.	3.6	18
151	Structural and optical studies of ZnAl 2 O 4 :x% Cu 2+ <mml:math xmlns:mml="http://www.w3.org/1998/Math/MathML" altimg="si1.gif" overflow="scroll"><mml:mrow><mml:mrow><mml:mo>(</mml:mo><mml:mrow><mml:mn>0</mml:mn><mml: synthesized via citrate sol-gel route. Optical Materials. 2017. 64. 26-32.</mml: </mml:mrow></mml:mrow></mml:mrow></mml:math 	mo ^{3.} <<	/mml:mo> <m< td=""></m<>
152	Physical and optical properties of lithium borosilicate glasses doped with Dy 3+ ions. Physica B: Condensed Matter, 2018, 535, 194-197.	2.7	18
153	Persistent photoluminescence emission from SrTa2O6:Pr3+ phosphor prepared at different temperatures. Ceramics International, 2015, 41, 8828-8836.	4.8	17
154	The effect of annealing temperature on the luminescence properties of Y2O3 phosphor powders doped with a high concentration of Bi3+. Journal of Luminescence, 2016, 180, 198-203.	3.1	17
155	The effect of different annealing temperatures on the structure and luminescence properties of Y2O3:Bi3+ thin films fabricated by spin coating. Applied Surface Science, 2016, 365, 93-98.	6.1	17
156	Photon and electron beam pumped luminescence of Ho3+ activated CaMoO4 phosphor. Applied Surface Science, 2017, 423, 1169-1175.	6.1	17
157	Self-assembled Cu doped CdS nanostructures on flexible cellulose acetate substrates using low cost sol–gel route. Nano Structures Nano Objects, 2018, 16, 1-8.	3.5	17
158	Effect of oxygen partial pressure during pulsed laser deposition on the emission of Eu doped ZnO thin films. Physica B: Condensed Matter, 2020, 576, 411713.	2.7	17
159	Characterization of the incorporated ZnO doped and co-doped with Ce3+ and Eu3+ nanophosphor powders into PVC polymer matrix. Journal of Molecular Structure, 2020, 1202, 127339.	3.6	17
160	Photoactive CdO:TiO2 nanocomposites for dyes degradation under visible light. Materials Chemistry and Physics, 2020, 253, 123191.	4.0	17
161	Thermally induced structural metamorphosis of ZnO:Rb nanostructures for antibacterial impacts. Colloids and Surfaces B: Biointerfaces, 2020, 188, 110821.	5.0	17
162	Effects of SnO2 surface coating on the degradation of ZnS thin film phosphor. Applied Surface Science, 2007, 253, 8513-8516.	6.1	16

#	Article	IF	CITATIONS
163	Characterization of Y2SiO5:Ce thin films. Optical Materials, 2007, 29, 1338-1343.	3.6	16
164	Surface chemical changes of CaTiO3:Pr3+ upon electron beam irradiation. Physica B: Condensed Matter, 2012, 407, 1517-1520.	2.7	16
165	Improved luminescence properties of pulsed laser deposited Y3(Al,Ga)5O12:Tb thin films by post deposition annealing. Journal of Luminescence, 2013, 143, 201-206.	3.1	16
166	Role of deposition time on the properties of ZnO:Tb3+ thin films prepared by pulsed laser deposition. Journal of Colloid and Interface Science, 2016, 474, 129-136.	9.4	16
167	Host sensitized near-infrared emission in Nd 3+ doped different alkaline-sodium-phosphate phosphors. Physica B: Condensed Matter, 2018, 535, 29-34.	2.7	16
168	Structural and luminescence properties of Y2O3:Eu3+red phosphor by incorporation of Ga3+ and Bi3+ions. Materials Research Bulletin, 2020, 124, 110752.	5.2	16
169	Degradation of ZnS:Cu,Al,Au phosphor powder in different gas mixtures. Journal of Luminescence, 2004, 109, 93-102.	3.1	15
170	The effect of different substrate temperatures on the structure and luminescence properties of Y2O3:Bi3+ thin films. Solid State Sciences, 2016, 53, 30-36.	3.2	15
171	x% Cr3+ <mml:math altimg="<sup" xmlns:mml="http://www.w3.org/1998/Math/MathML">"si1.gif" overflow="scroll"> <mml:mrow> <mml:mo stretchy="true"> (<mml:mrow> <mml:mn>0</mml:mn> <mml:mo> ≤/mml:mo> <mml:mi>x<td>> 29 ≻ 2mml:m</td><td>o>≤/mml:</td></mml:mi></mml:mo></mml:mrow></mml:mo </mml:mrow></mml:math>	> 2 9 ≻ 2 mml:m	o>≤/mml:
172	Optik, 2017, 131, 705-712. Analysis of the electron-vibrational interaction in the 5d states of Eu2+ ions in LiSrPO4 host matrix. Journal of Luminescence, 2019, 214, 116564.	3.1	15
173	Evaluation of the effects of Au addition into ZnFe2O4 nanostructures on acetone detection capabilities. Materials Research Bulletin, 2021, 142, 111395.	5.2	15
174	Luminescence and electron degradation properties of Bi doped CaO phosphor. Applied Surface Science, 2015, 356, 1064-1069.	6.1	14
175	The effect of different annealing temperatures on the structure and luminescence properties of Y 2 O 3 :Bi 3+ thin film fabricated by RF magnetron sputtering. Applied Surface Science, 2017, 424, 407-411.	6.1	14
176	Cathodoluminescence degradation study of the green luminescence of ZnO nanorods. Applied Surface Science, 2019, 484, 105-111.	6.1	14
177	Structural, luminescent and thermal properties of blue SrAl2O4:Eu2+, Dy3+ phosphor filled low-density polyethylene composites. Physica B: Condensed Matter, 2009, 404, 4504-4508.	2.7	13
178	Characterization of luminescent and thermal properties of long afterglow SrAlxOy:Eu ²⁺ ,Dy ³⁺ phosphor synthesized by combustion method. Polymer Composites, 2011, 32, 219-226.	4.6	13
179	Surface characterization and luminescent properties of SrAl2O4:Eu2+, Dy3+ nano thin films. Physica B: Condensed Matter, 2012, 407, 1660-1663.	2.7	13
180	Synthesis and characterization of Y2O3:Eu3+ phosphors using the Sol-Combustion method. Physica B: Condensed Matter, 2014, 439, 181-184.	2.7	13

#	Article	IF	CITATIONS
181	Comparison of Y2O3:Bi3+ phosphor thin films fabricated by the spin coating and radio frequency magnetron techniques. Physica B: Condensed Matter, 2016, 497, 39-44.	2.7	13
182	Luminescence properties of Eu doped ZnO PLD thin films: The effect of oxygen partial pressure. Superlattices and Microstructures, 2020, 139, 106432.	3.1	13
183	The influence of sulphur segregation on the oxidation of industrial FeCrMo steel. Corrosion Science, 2000, 42, 991-1004.	6.6	12
184	Photon emission mechanisms of different phosphors. Nuclear Instruments & Methods in Physics Research B, 2009, 267, 2630-2633.	1.4	12
185	Lattice site dependent cathodoluminescence behavior and surface chemical changes in a Sr5(PO4)3F host. Physica B: Condensed Matter, 2012, 407, 1505-1508.	2.7	12
186	Luminescence studies of a combustion-synthesized blue–green BaAlxOy:Eu2+,Dy3+ nanoparticles. Physica B: Condensed Matter, 2012, 407, 1561-1565.	2.7	12
187	Sensitizing effects of ZnO quantum dots on red-emitting Pr3+-doped SiO2 phosphor. Physica B: Condensed Matter, 2012, 407, 1607-1610.	2.7	12
188	A comparative study of the effect of Ni9+ and Au8+ ion beams on the properties of poly(methacrylic) Tj ETQqO C	0 rgBT /O	verlock 10 Th
189	Characterization of crystallite morphology for doped strontium fluoride nanophosphors by TEM and XRD. Physica B: Condensed Matter, 2016, 480, 169-173.	2.7	12
190	Investigation of thermoluminescence characteristics of NaSrBO 3 :Sm 3+ phosphor against 120 MeV Ag 9+ ion and γ-ray irradiation prepared by different methods. Journal of Luminescence, 2017, 187, 499-506.	3.1	12
191	Red emitting non-rare earth doped LiMgBO3 phosphor for light emitting diodes. Journal of Alloys and Compounds, 2020, 830, 154622.	5.5	12
192	Luminescence response and CL degradation of combustion synthesized spherical SiO2:Ce nanophosphor. Materials Research Bulletin, 2011, 46, 2359-2366.	5.2	11
193	Luminescence from Ce in sol–gel SiO2. Physica B: Condensed Matter, 2012, 407, 1595-1598.	2.7	11
194	Luminescent properties and quenching effects of Pr3+ co-doping in SiO2:Tb3+/Eu3+ nanophosphors. Optical Materials, 2014, 36, 732-739.	3.6	11
195	Optical and Chemical Properties of Alq3:PMMA Blended Thin Films. Materials Today: Proceedings, 2015, 2, 4019-4027.	1.8	11
196	Thermoluminescence response of 120 MeV Ag9+ and γ-ray exposed LiMgBO3:Dy3+ nanophosphors for dosimetry. Ceramics International, 2016, 42, 18529-18535.	4.8	11
197	Luminescence properties of Y 2 O 3 :Bi 3+ , Yb 3+ co-doped phosphor for application in solar cells. Physica B: Condensed Matter, 2018, 535, 102-105.	2.7	11
198	Comparative study of photo- and non-photo-assisted chemical bath deposition of Zinc Selenide thin films using different volumes of hydrazine hydrate. Superlattices and Microstructures, 2019, 134, 106222.	3.1	11

#	Article	IF	CITATIONS
199	Synthesis and characterization of europium doped zinc selenide thin films prepared by photo-assisted chemical bath technique for luminescence application. Materials Chemistry and Physics, 2021, 262, 124303.	4.0	11
200	Study of photoluminescence and nonlinear optical behaviour of AgCu nanoparticles for nanophotonics. Nano Structures Nano Objects, 2021, 28, 100807.	3.5	11
201	A comparative study between the simulated and measured cathodoluminescence generated in ZnS:Cu, Al, Au phosphor powder. Journal of Luminescence, 2005, 113, 191-198.	3.1	10
202	Effects of Ce3+ concentration, beam voltage and current on the cathodoluminescence intensity of SiO2:Pr3+–Ce3+ nanophosphor. Journal of Alloys and Compounds, 2011, 509, 2986-2992.	5.5	10
203	Dependence of luminescence properties of CaTiO3:Pr3+ on different TiO2 polymorphs. Powder Technology, 2014, 256, 477-481.	4.2	10
204	Structural and morphology analysis of annealed Y3(Al,Ga)5O12:Tb thin films synthesized by pulsed laser deposition. Applied Surface Science, 2014, 305, 732-739.	6.1	10
205	Near infrared quantum cutting of Na + and Eu 2+ -Yb 3+ couple activated SrF 2 crystal. Optical Materials, 2016, 60, 521-525.	3.6	10
206	Effect of swift heavy ion irradiation on structural, optical and luminescence properties of SrAl2O4:Eu2+, Dy3+ nanophosphor. Radiation Physics and Chemistry, 2016, 122, 48-54.	2.8	10
207	Surface characterization of ZnO nanorods grown by chemical bath deposition. Physica B: Condensed Matter, 2016, 480, 42-47.	2.7	10
208	Optical properties and stability of Bi doped La2O2S. Optical Materials, 2019, 95, 109260.	3.6	10
209	Cathodoluminescence degradation of Bi doped La2O3 and La2O2S phosphor powders. Physica B: Condensed Matter, 2019, 574, 411659.	2.7	10
210	The role of sulfate ions on distinctive defect emissions in ZnO:Ce3+ nanophosphors - A study on the application in color display systems. Journal of Luminescence, 2021, 240, 118462.	3.1	10
211	Low temperature effect on the electron beam induced degradation of ZnS:Cu,Al,Au phosphor powders. Applied Surface Science, 2002, 193, 77-82.	6.1	9
212	Modelling the effect of a thin ZnO layer on the cathodoluminescence generated in ZnS phosphor powders. Thin Solid Films, 2002, 408, 260-269.	1.8	9
213	Effect of different annealing temperatures on the optical properties of Y3(Al,Ga)5O12:Tb thin films grown by PLD. Physica B: Condensed Matter, 2014, 439, 77-82.	2.7	9
214	The influence of Ag9+ ion irradiation on the structural, optical and luminescence properties of Sm3+ doped NaSrBO3: Stability of color emission. Nuclear Instruments & Methods in Physics Research B, 2015, 351, 27-34.	1.4	9
215	Trap characteristics of UV-activated Y3(Al,Ga)5O12:Ce3+ phosphors. Optik, 2016, 127, 3918-3924.	2.9	9
216	The influence of substrate temperature and deposition pressure on pulsed laser deposited thin films of CaS:Eu2+ phosphors. Physica B: Condensed Matter, 2016, 480, 186-190.	2.7	9

#	Article	IF	CITATIONS
217	Effect of Yb 3+ ions on structural and NIR emission of SrF 2 :Eu 2+ /Pr 3+ down-conversion containing Na + ions. Materials Research Bulletin, 2017, 93, 170-176.	5.2	9
218	Photoluminescence, thermoluminescence and defect centres in Y2O3 and Y2O3:Tb3+ under 100†MeV swift Ni8+ ion beam irradiation. Materials Research Bulletin, 2018, 102, 62-69.	5.2	9
219	A potential green emitting citrate gel synthesized NaSrBO 3 :Tb 3+ phosphor for display application. Physica B: Condensed Matter, 2018, 535, 189-193.	2.7	9
220	Surface and chemical characterization of ZnO:Eu3+/Yb3+ spin coated thin films using SEM-CL and TOF-SIMS. Vacuum, 2018, 157, 376-383.	3.5	9
221	The effect of pH on the luminescence properties of Y2O3:Bi phosphor powders synthesised using co-precipitation. Vacuum, 2018, 157, 237-242.	3.5	9
222	Thermoluminescence response in 60Co gamma rays, 100†MeV Si8+ and 150†MeV Au9+ irradiated Y2O3:Ho nanophosphor. Journal of Alloys and Compounds, 2019, 778, 554-565.	3+ _{5.5}	9
223	Electron beam induced green luminescence and degradation study of CaS:Ce nanocrystalline phosphors for FED applications. Applied Surface Science, 2010, 256, 1720-1724.	6.1	8
224	Improvement of the photoluminescent intensity of ZnTa2O6:Pr3+ phosphor. Materials Research Bulletin, 2014, 55, 150-155.	5.2	8
225	Structural and luminescence properties of SrAl2O4:Eu2+,Dy3+,Nd3+ phosphor thin films grown by pulsed laser deposition. Physica B: Condensed Matter, 2016, 480, 116-124.	2.7	8
226	Colour tuneable emission from (Y1.995â^'xGax)2O3:Bi3+ phosphor prepared by a sol-gel combustion method. Materials Letters, 2017, 186, 345-348.	2.6	8
227	Energy transfer upconversion in Er 3+ -Tm 3+ codoped sodium silicate glass. Physica B: Condensed Matter, 2018, 535, 330-332.	2.7	8
228	Upconversion process in BaY ₂ F ₈ :Yb ³⁺ ,Ho ³⁺ phosphor for optical thermometry. Luminescence, 2021, 36, 1847-1850.	2.9	8
229	Phase transformation on zinc selenide thin films deposited by photo-assisted chemical bath method: The effect of annealing temperature. Materials Science in Semiconductor Processing, 2020, 115, 105118.	4.0	8
230	Color tuning of the Ba1.96Mg(PO4)2:0.04Eu2+ phosphor induced by the chemical unit co-substitution of the (BO3)3â^' anion group. Journal of Alloys and Compounds, 2021, 864, 158124.	5.5	8
231	Structural, surface and luminescent properties of SrF2:Eu annealed thin films. Vacuum, 2021, 191, 110362.	3.5	8
232	Luminescent behaviour of SrF2 and CaF2 crystals doped with Eu ions under different annealing temperatures. Journal of Alloys and Compounds, 2021, 858, 157741.	5.5	7
233	Characteristic properties of Y2SiO5:Ce thin films grown with PLD. Physica B: Condensed Matter, 2009, 404, 4431-4435.	2.7	6
234	Ion-induced modification of structural, optical and luminescence behaviour of Gd2MoO6 nanomaterials: A comparative approach. Vacuum, 2016, 128, 146-157.	3.5	6

#	Article	IF	CITATIONS
235	Upconversion luminescence of Er 3+ /Yb 3+ doped Sr 5 (PO 4) 3 OH phosphor powders. Physica B: Condensed Matter, 2018, 535, 57-62.	2.7	6
236	Development of an optical thermometry system for phosphor materials. Vacuum, 2018, 155, 702-711.	3.5	6
237	Photoluminescence and thermoluminescence studies of 100†MeV Si8+ ion irradiated Y2O3:Dy3+ nanophosphor. Journal of Luminescence, 2019, 209, 179-187.	3.1	6
238	Effect of hydrazine hydrate as complexing agent in the synthesis of zinc selenide thin films by chemical bath deposition. Thin Solid Films, 2020, 693, 137707.	1.8	6
239	Electron Beam Degradation of Sulfide-Based Thin-Film Phosphors for Field Emission Flat Panel Displays. Materials Research Society Symposia Proceedings, 1998, 508, 261.	0.1	5
240	The effect of the host lattice on the optical properties of Bi 3+ in Ca 1-x O:Bi and Ca 1-x (OH) 2 :Bi phosphors. Applied Surface Science, 2018, 433, 155-159.	6.1	5
241	Structural, morphological and optical properties of ZnO nanorods grown on a ZnO:Ga seeded thin film: The role of chemical bath deposition precursor concentration at constant and varying II/VI molar ratios. Thin Solid Films, 2019, 687, 137483.	1.8	5
242	Blue-emitting Ca3Mg3(PO4)4:Eu2+ phosphor: Study of electron-vibrational interaction in the 5d states of Eu2+ ions. Optical Materials, 2021, 114, 110959.	3.6	5
243	Electron beam irradiation studies of ZnGa2O4:Mn2+ green phosphor. Vacuum, 2021, 192, 110447.	3.5	5
244	Thermo-luminescence kinetic parameters of γ-irradiated Sr ₄ Al ₁₄ O ₂₅ :Eu ²⁺ , Dy ³⁺ phosphors. Radiation Effects and Defects in Solids, 2013, 168, 1022-1029.	1.2	4
245	The influence of laser wavelength on the structure, morphology, and photoluminescence properties of pulsed laser deposited CaS: Eu2+thin films. Journal of Modern Optics, 2015, 62, 1102-1109.	1.3	4
246	Photoluminescence and thermoluminescence properties of Y3(Al,Ga)5O12:Tb3+phosphor. Journal of Modern Optics, 2016, 63, 103-110.	1.3	4
247	Controlling the morphology of ZnO NRs grown on GZO seed layer, by use of ethylenediamine and L-cysteine as crystal growth modifiers and complexing agents. Applied Surface Science, 2019, 487, 1198-1208.	6.1	4
248	Luminescence of Alternating SiO2:Tb and SiO2:Ce Thin Films Produced by Sol-gel Spin Coating. Materials Today: Proceedings, 2015, 2, 4111-4117.	1.8	3
249	Ag7+ ion induced modification of morphology, optical and luminescence behaviour of charge compensated CaMoO4 nanophosphor. Nuclear Instruments & Methods in Physics Research B, 2016, 384, 76-85.	1.4	3
250	Structural and optical characterization of mechanically milled Mg-TiO2 and nitrided Mg-TiO -N nanostructures: Possible candidates for gas sensing application. Applied Surface Science, 2016, 360, 1047-1058.	6.1	3
251	Structure and photoluminescence properties of Ba 2â^'x Si 4 O 10 :2xSm 3+. Physica B: Condensed Matter, 2018, 535, 50-56.	2.7	3
252	Structural and Luminescence Properties of ZnO Nanoparticles Synthesized by Mixture of Fuel		3

#	Article	IF	CITATIONS
253	Interface analysis of SrWO4:Er3+-Yb3+/Si thin films prepared by radio frequency magnetron sputtering for upconversion emission. Physica B: Condensed Matter, 2021, 623, 413349.	2.7	3
254	Photoluminescence, cathodoluminescence degradation and surface analysis of Gd2O3:Bi pulsed laser deposition thin films. Physica B: Condensed Matter, 2022, 631, 413618.	2.7	3
255	Investigation of ageing characteristics and identification of surface chemical changes on SrGa2S4:Ce3+ display phosphor under electron beam bombardment. Physica B: Condensed Matter, 2012, 407, 1645-1648.	2.7	2
256	La 3+ eliminate the blue component from the emission of Y 2 O 3 : Bi 3+. Materials Letters, 2016, 171, 171-173.	2.6	2
257	Compound Luminescent Semiconductors: Their Properties and Uses. , 2013, , 73-86.		1
258	Role of Ga particulates on the structure and optical properties of Y 3 (Al,Ga) 5 O 12 :Tb thin films prepared by PLD. Physica B: Condensed Matter, 2018, 535, 319-322.	2.7	1
259	Synthesis of silver incorporated lithium doped zinc oxide nanocomposites for in-vitro biorational evaluation of Candiasis and Cryptococcosis. Applied Surface Science, 2020, 506, 144800.	6.1	1
260	The morphology and downshifting luminescence of [CaY]F2 crystals doped with Ce3+/Eu3+/2+/Na+. Ceramics International, 2022, 48, 23657-23665.	4.8	1
261	Energy transfer mechanism in Eu3+ doped tin oxide nanophosphors for red solid state lighting. Journal of Luminescence, 2022, 250, 119085.	3.1	1